

Refining Gravitational Wave and Collider Physics Dialogue via Singlet Scalar Extension

Van Que Tran

NCTS, National Taiwan University

In collaboration: **Michael J. Ramsey-Musolf, Tuomas V. I. Tenkanen**

Based on: [arXiv:2409.17554](https://arxiv.org/abs/2409.17554)

Summer Institute 2025

@Yeosu, Korea, Aug. 17-22, 2025



National Center for Theoretical Sciences

Physics Division 國家理論科學研究中心 物理組



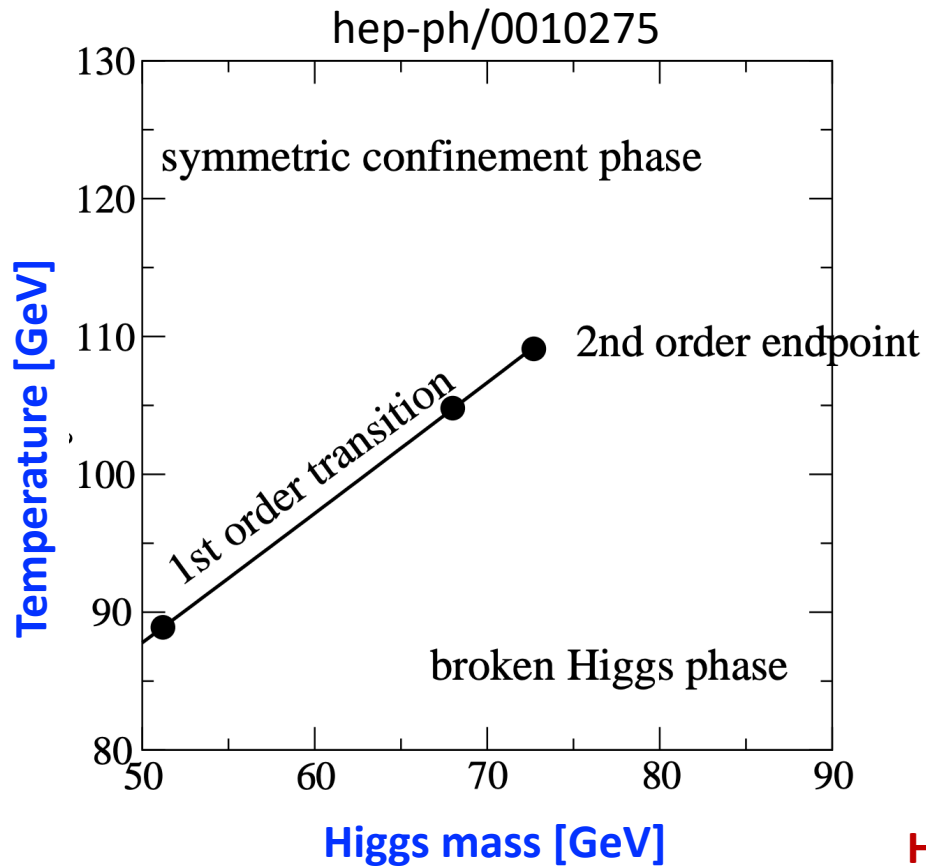
I. Introduction

II. Theoretical Robustness on GW prediction

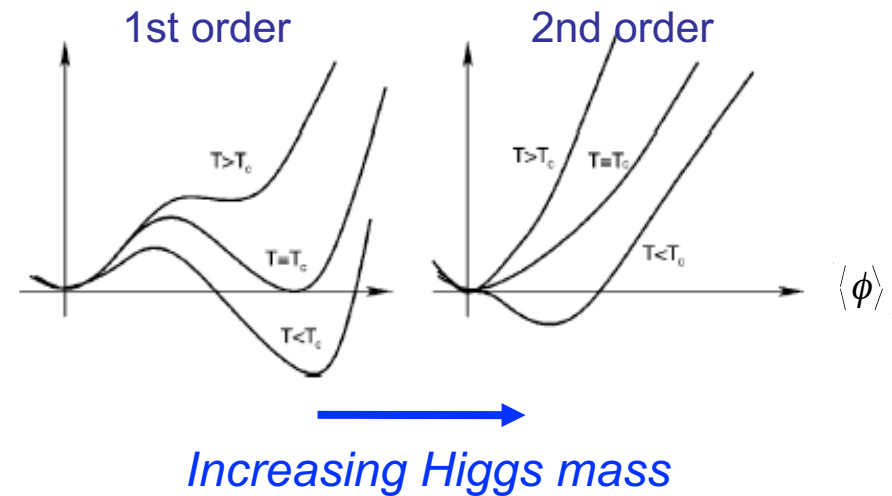
- Dimensional reduction (3dEFT)
- Higher loop corrections
- Bubble wall velocity

III. GW-Collider interplays via xSM

IV. Summary



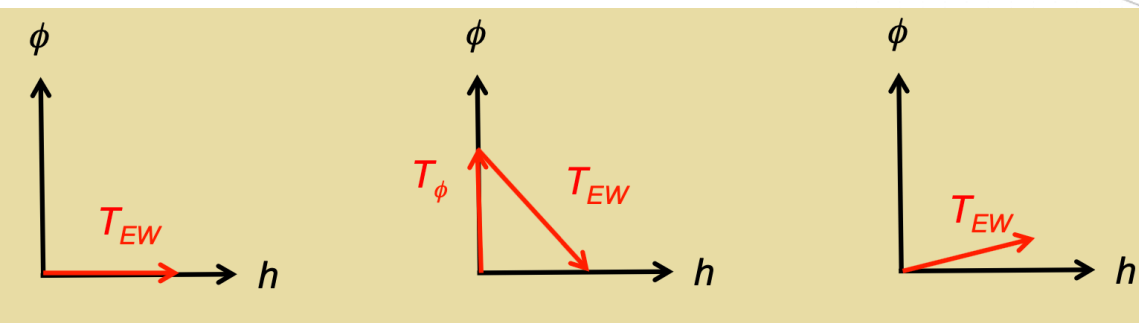
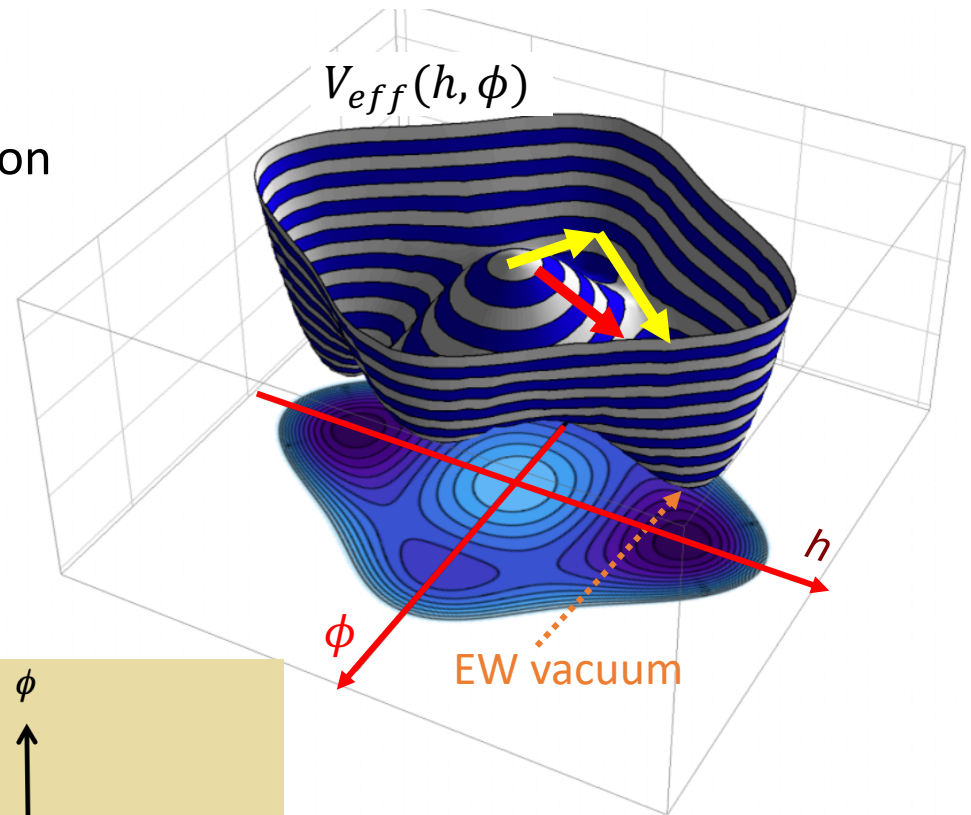
EW Phase Diagram

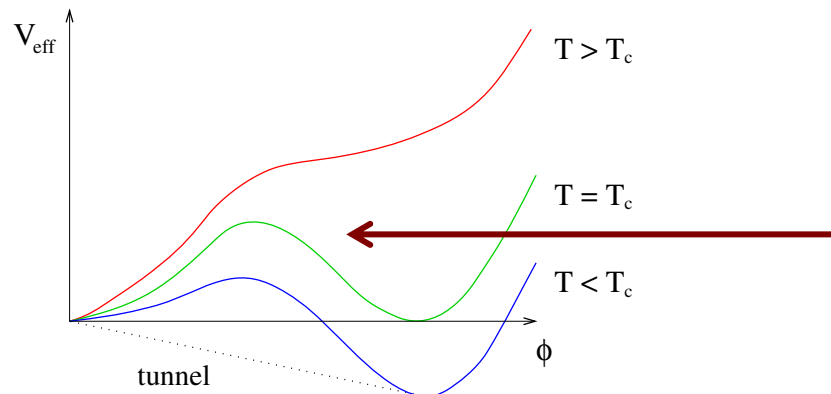


Higgs mass: 125 GeV

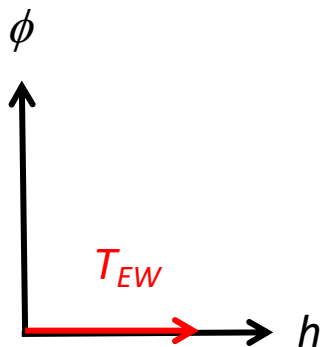
→ SM EW transition is a **crossover**

- Effective potential a function of multiple order parameters.
- Possible of multi-step phase transition

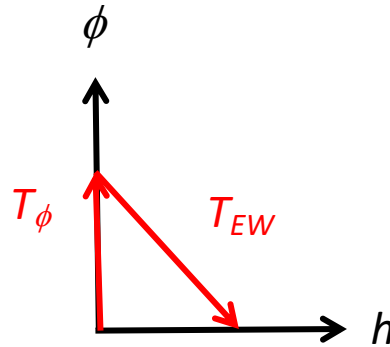




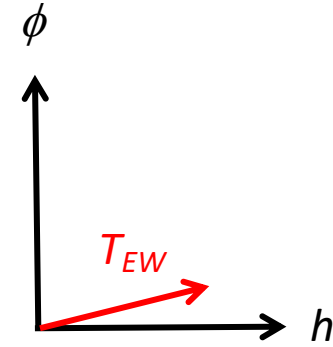
Generate finite- T barrier



$a_2 H^2 \phi^2 : T > 0$
loop effect



$a_2 H^2 \phi^2 : T = 0$
tree-level effect



$a_1 H^2 \phi : T = 0$
tree-level effect



1st order EW phase transition is interesting?

1. It can be indirectly probed by collider
2. It can generate a stochastic background of GW which can be detectable by the next generation of GW detectors such as LISA.
3. It is one of necessary preconditions (Sakharov conditions) for the generation of the observed baryon asymmetry via electroweak baryogenesis



How reliable are the computations for GW predictions?

- Temperature T_* :

➤ $T_* \sim 100 \text{ GeV} \rightarrow \text{mHz today}$

- Latent heat or phase transition strength, α

$$\alpha = \frac{\rho_{\text{vac}}}{\rho_{\text{rad}}^*} = \frac{1}{\rho_{\text{rad}}^*} \left[\frac{1}{4} T \frac{\partial}{\partial T} \Delta V(T) - \Delta V(T) \right] \Big|_{T_*}$$

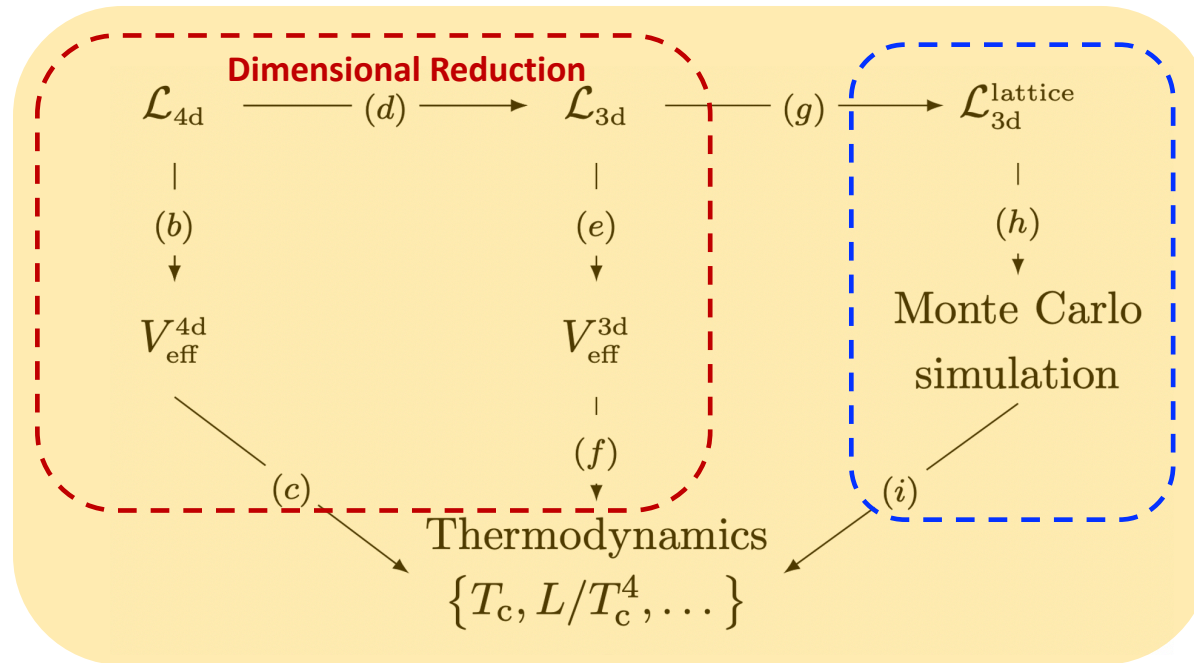
- “Duration”:

$$\frac{\beta}{H_*} = -T \frac{d}{dT} \ln \Gamma \Big|_{T=T_*}$$

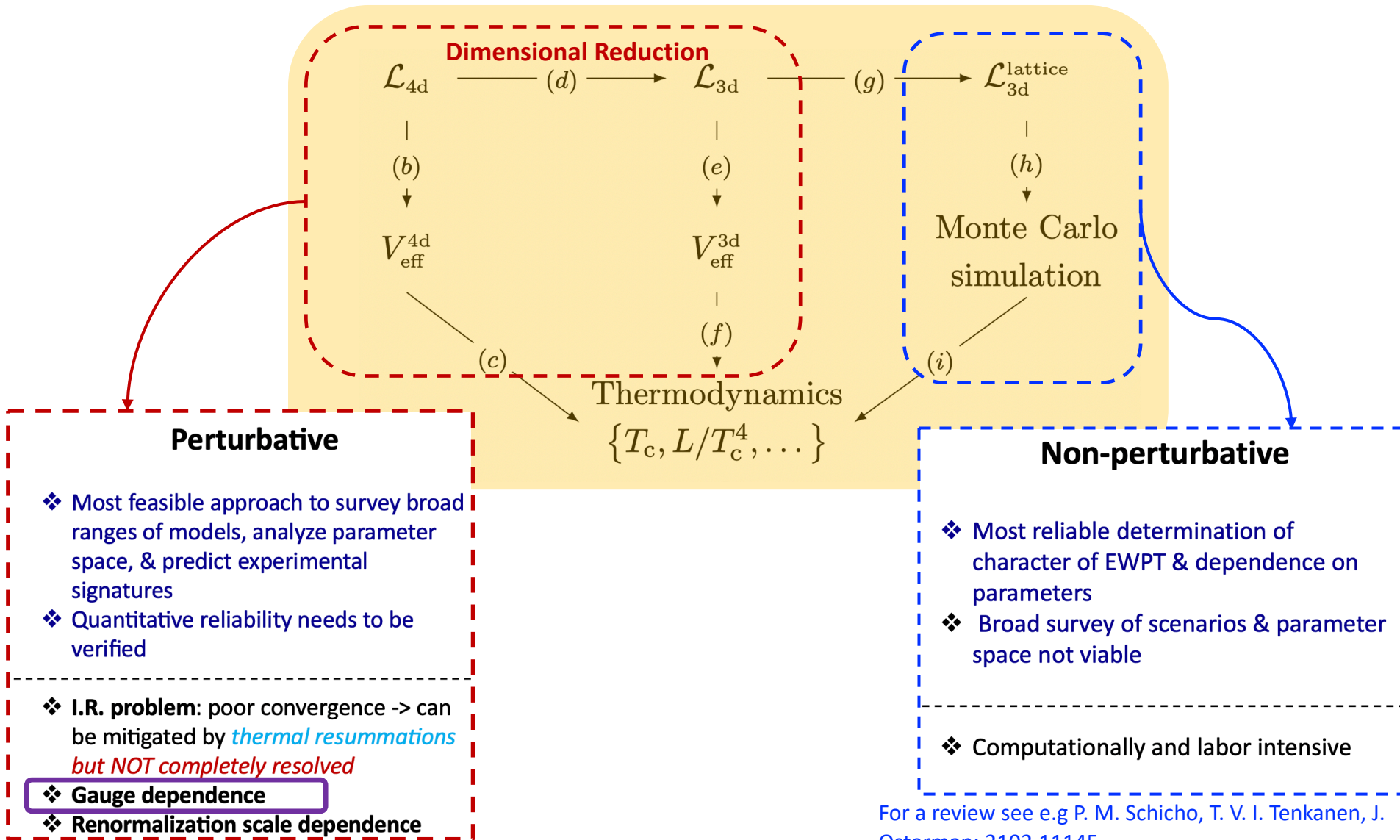
β : inverse phase transition duration

H_* : Hubble rate at transition

- v_w : bubble wall velocity



For a review see e.g P. M. Schicho, T. V. I. Tenkanen, J. Osterman: 2102.11145



For a review see e.g. P. M. Schicho, T. V. I. Tenkanen, J. Osterman: 2102.11145

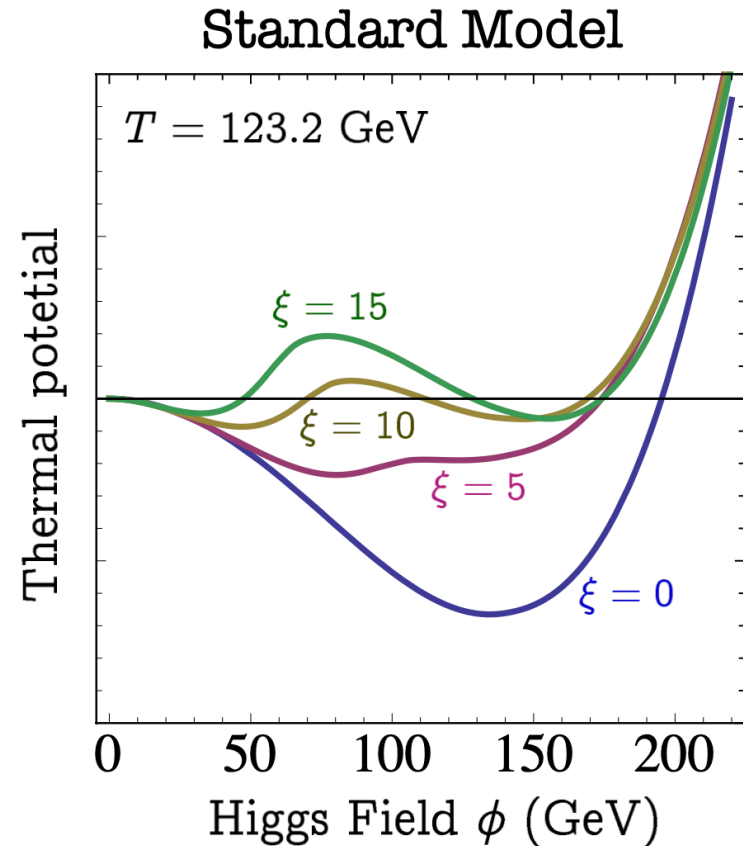


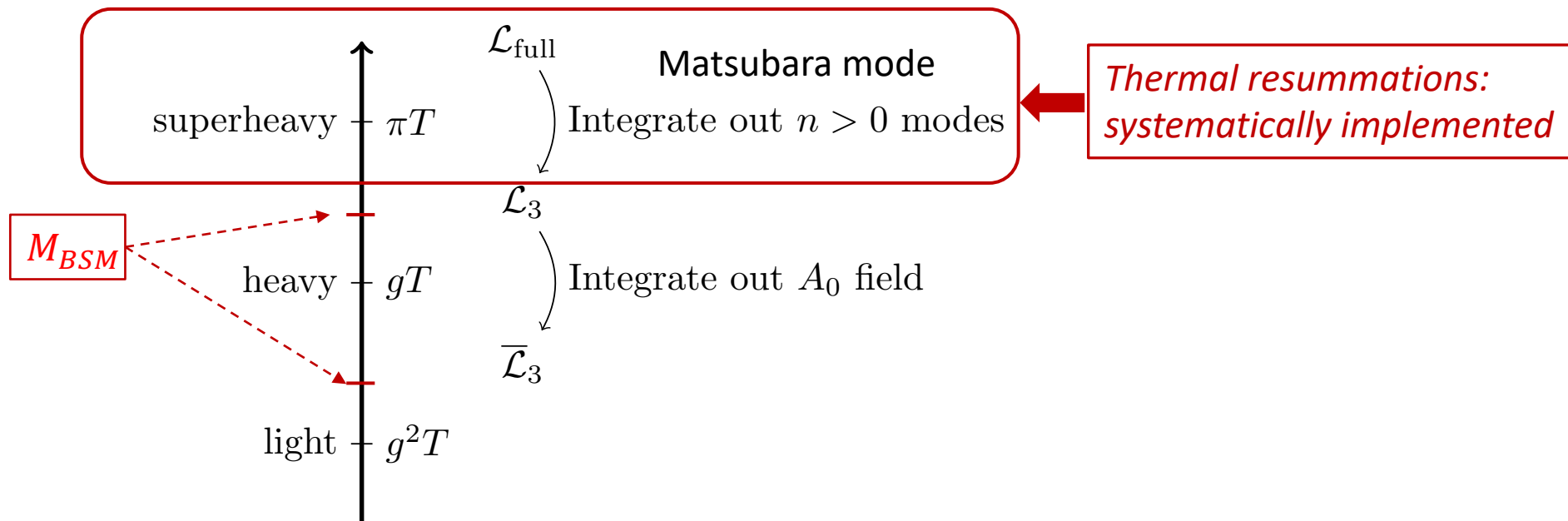
❖ The full effective potential depends on the gauge parameter

❖ Need to use approximations to obtain a gauge independent effective potential:

1. Using high-T expansion
2. Using \hbar expansion (PRM method)

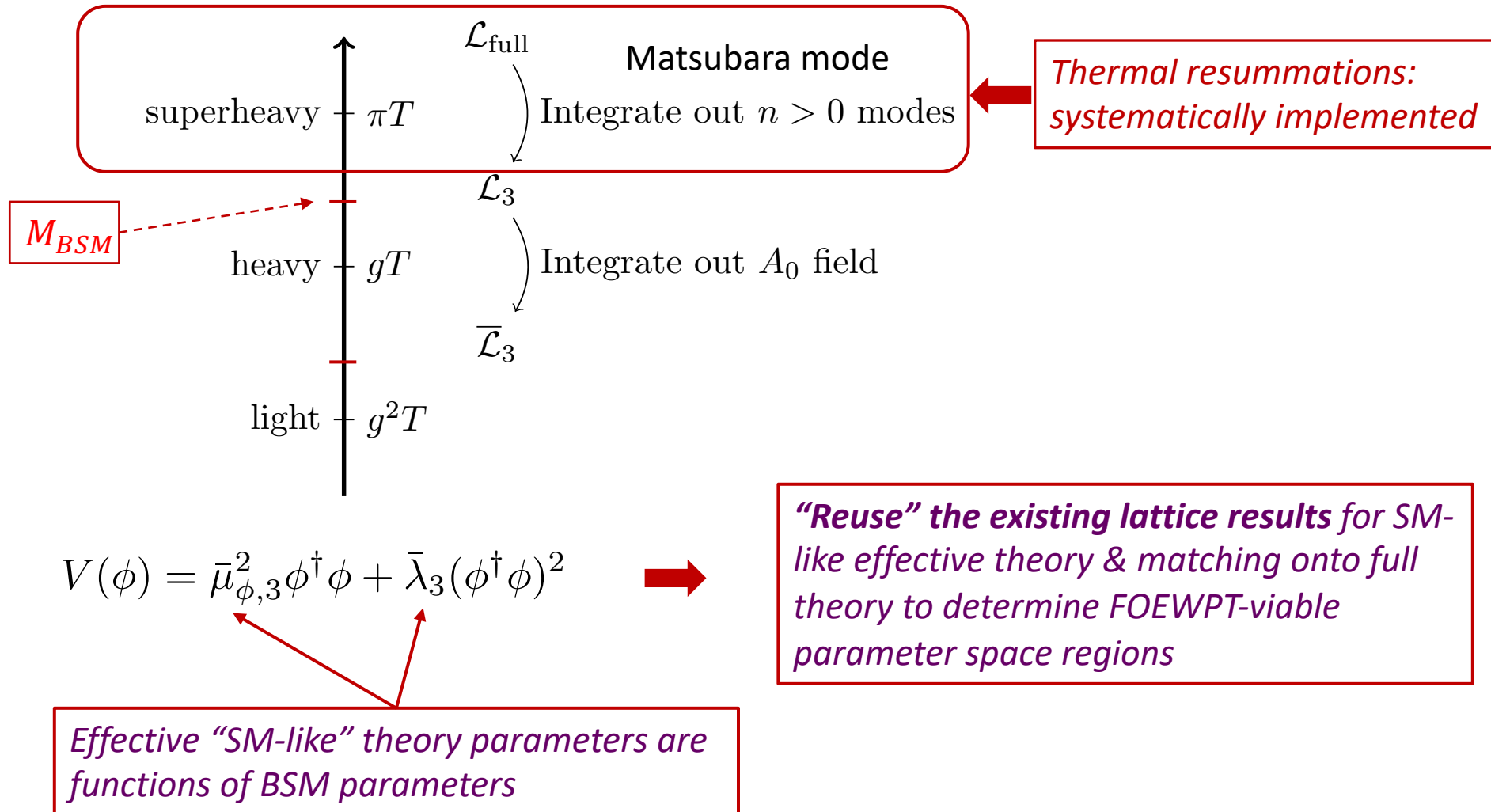
H.H.Patel and M.J.Ramsey-Musolf JHEP 07 (2011), 029, arXiv:1101.4665





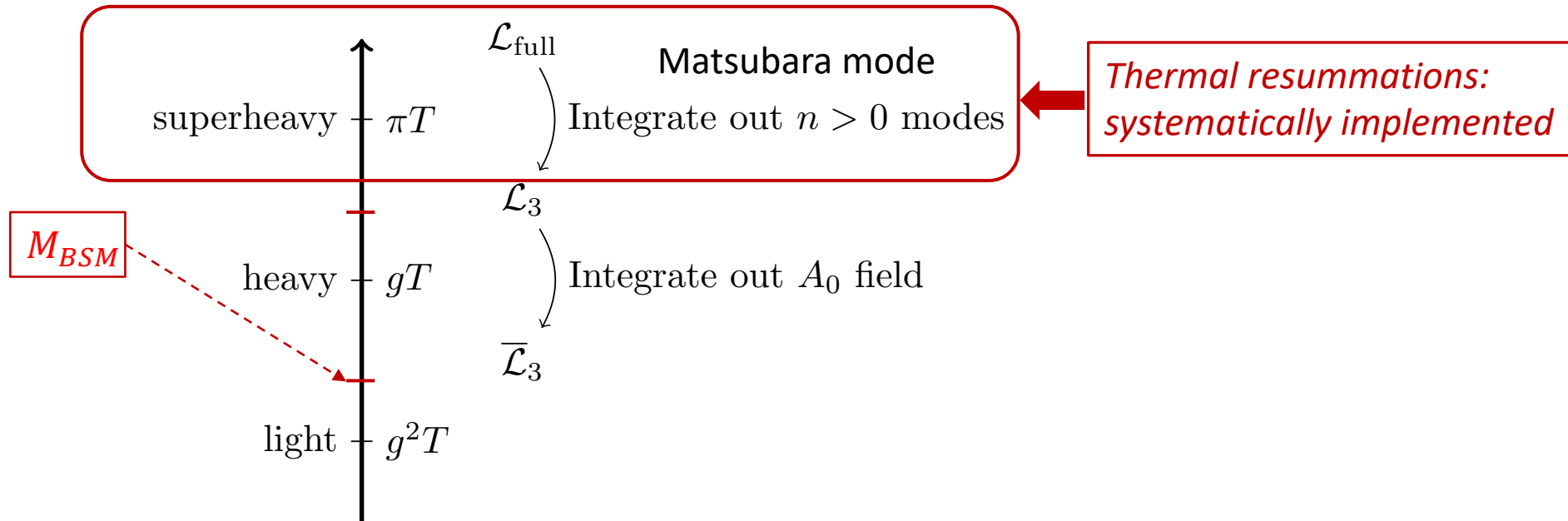


❖ Heavy BSM mass





❖ Light BSM mass



$$V(\phi) = \bar{\mu}_{\phi,3}^2 \phi^\dagger \phi + \bar{\lambda}_3 (\phi^\dagger \phi)^2 + V_{BSM}$$



Perform new lattice simulations

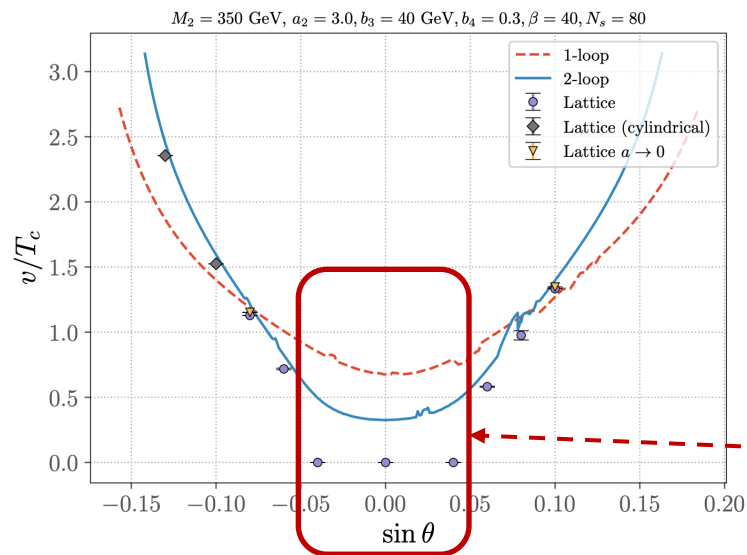
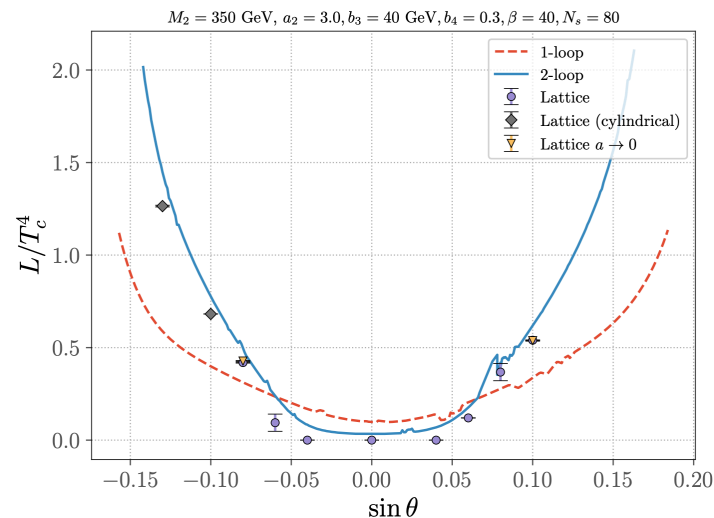
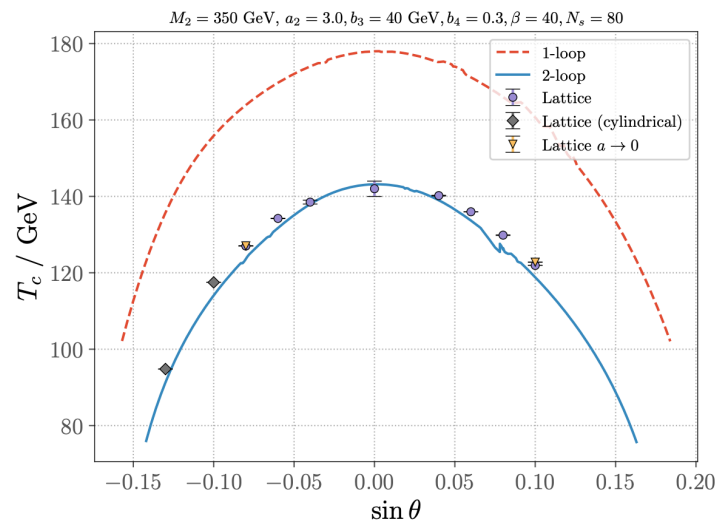
Effective “SM-like” theory parameters are functions of BSM parameters

For recent lattice simulations, see

- Niemi, Ramsey-Musolf, Tenkanen, Weir 2005.11332
- L. Niemi, Michael J. Ramsey-Musolf, G. Xia: 2405.01191



DR 3EFT perturbative vs Lattice: *singlet scalar extension*

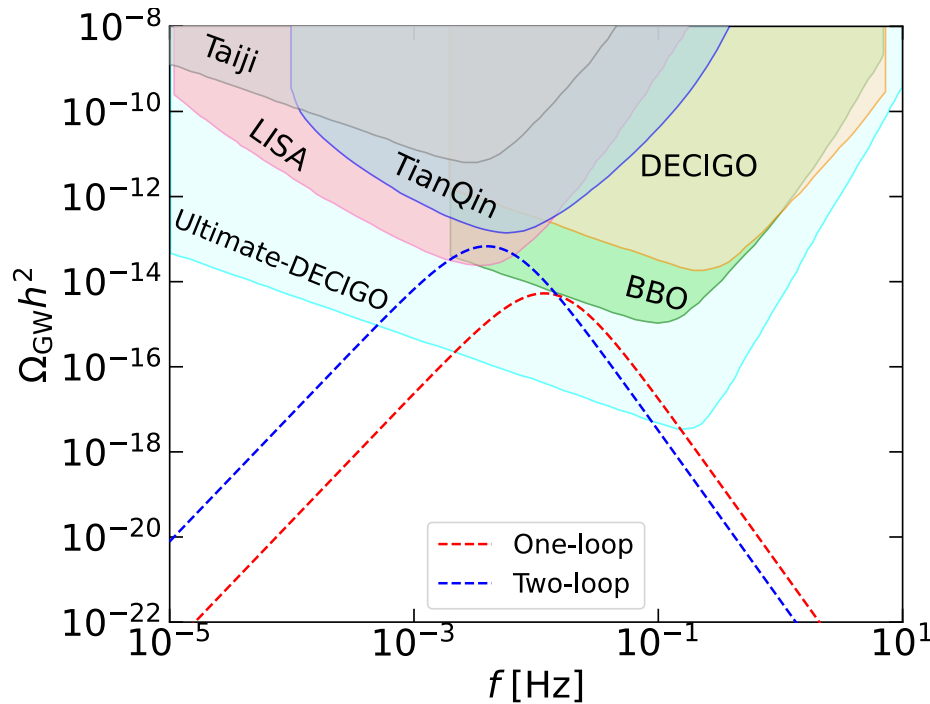


L. Niemi, M. J. Ramsey-Musolf, G. Xia: 2405.01191



DR 3EFT perturbative: GW spectrum from 1-loop vs 2-loop corrections

Ramsey-Musolf, Tenkanen, VQT: 2409.17554



Spectrum is obtained using
PTPlot package

BM: $m_{h_2} = 350$ GeV, $b_3 = 40$ GeV, $b_4 = 0.3$, $a_2 = 3.0$, and $\sin \theta = 0.1$.

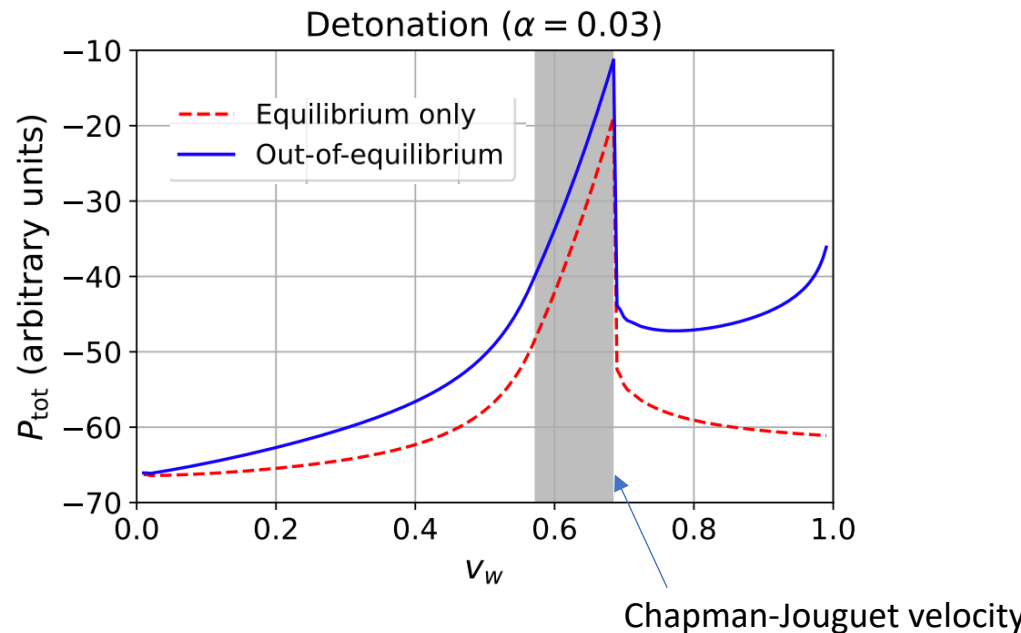
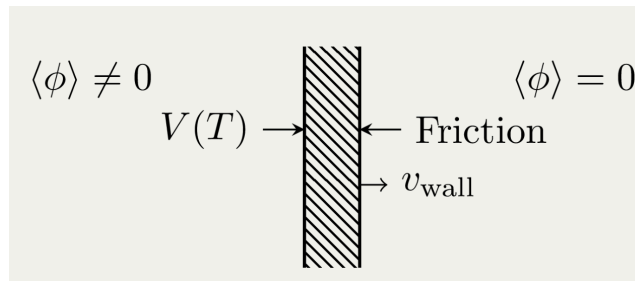
At one-loop order, we find

$$T_* = 82.12 \text{ GeV}, \quad \alpha = 0.065, \quad \frac{\beta}{H_*} = 1102.57, \quad v_w^{\text{LTE}} = 0.70, \quad \text{SNR}_{\text{LISA}} = 0.18.$$

Including two-loop corrections results:

$$T_* = 64.75 \text{ GeV}, \quad \alpha = 0.128, \quad \frac{\beta}{H_*} = 528.4, \quad v_w^{\text{LTE}} = 0.78, \quad \text{SNR}_{\text{LISA}} = 9.3.$$

- ❖ Computing bubble wall velocity is **challenging** especially including **out-of-equilibrium** effects <- *how the **plasma's distribution functions** are represented and calculated?*
- ❖ However, the out-of-equilibrium effects are typically **subdominant** for some BSMs!
- The wall velocity can be computed using **Local Thermal Equilibrium approximation***



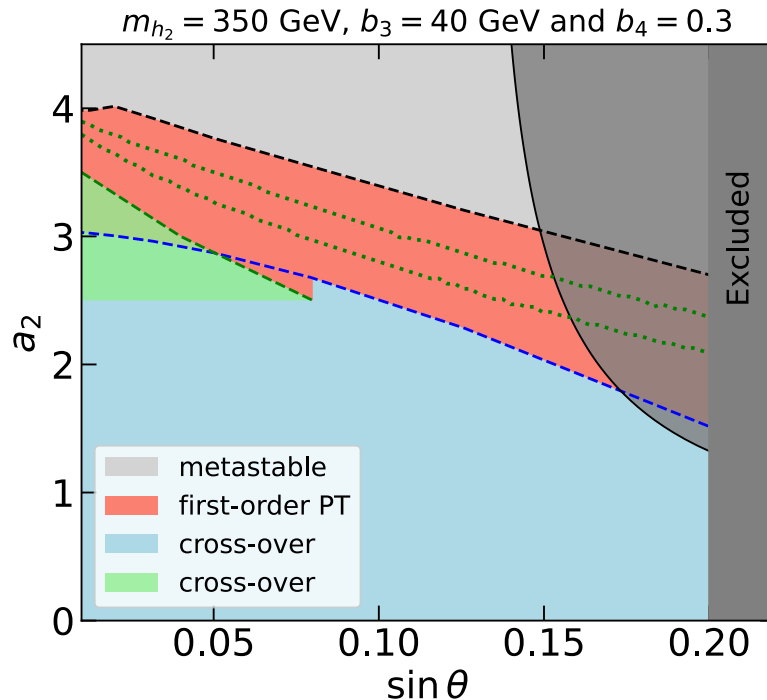
*all the species in the plasma are in local thermal equilibrium at the same temperature and fluid velocity

B. Laurent and J.M. Cline: 2204.13120

W-Y. Ai, B. Laurent and J. Vis: 2303.10171

Phase structure diagram

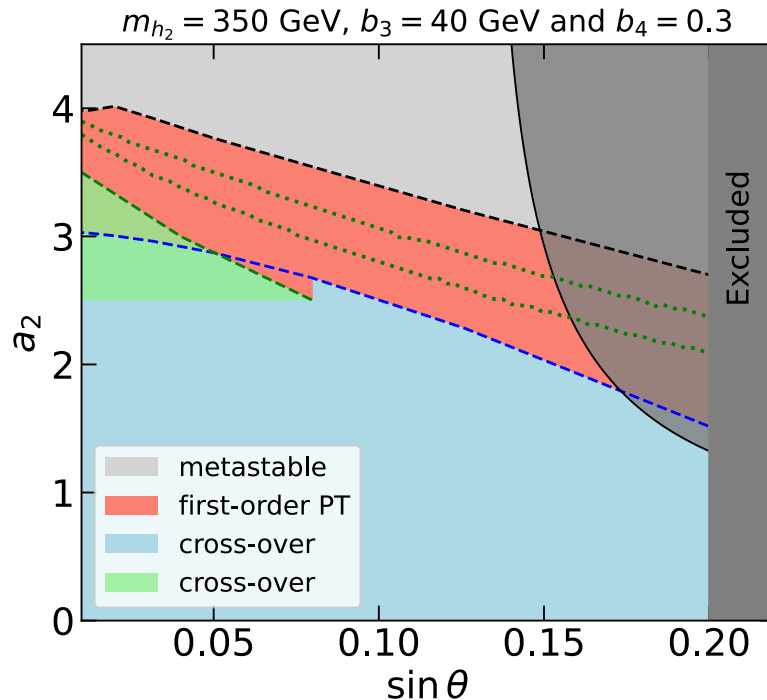
Ramsey-Musolf, Tenkanen, VQT: 2409.17554



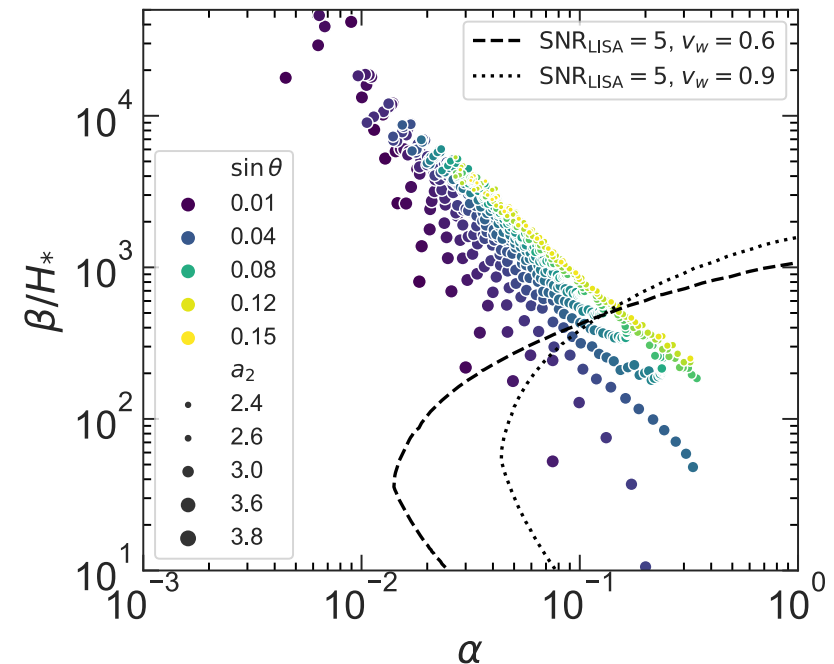
Crossover: assuming the singlet is **NOT** dynamical in the lattice simulation

Crossover: assuming the singlet is dynamical in the lattice simulation

Phase structure diagram



Ramsey-Musolf, Tenkanen, VQT: 2409.17554



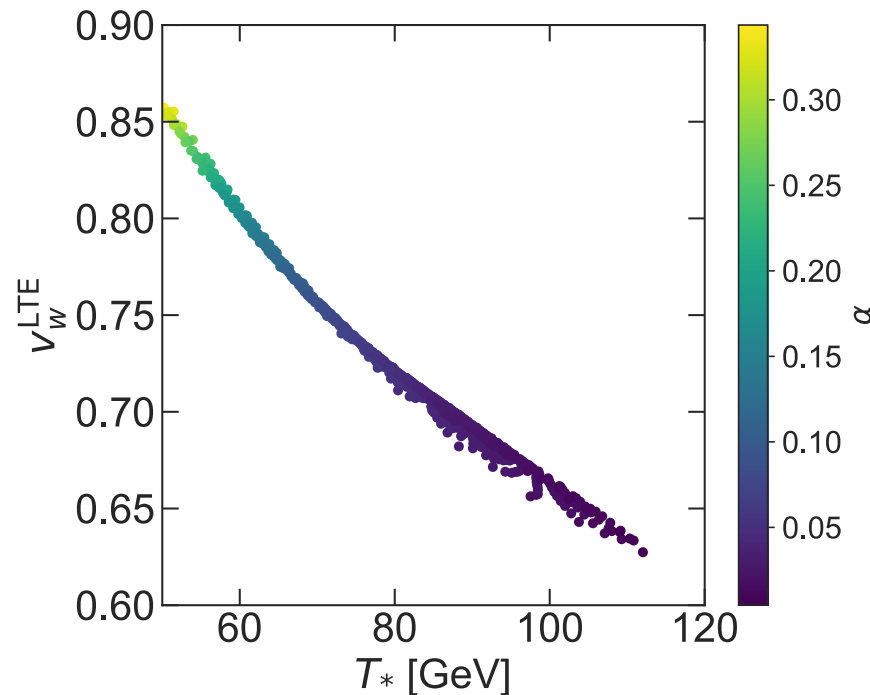
Crossover: assuming the singlet is **NOT** dynamical in the lattice simulation

Crossover: assuming the singlet is dynamical in the lattice simulation

The phase transition strength and its duration is sensitive to the coupling a_2 .

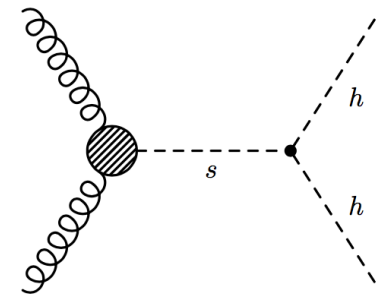
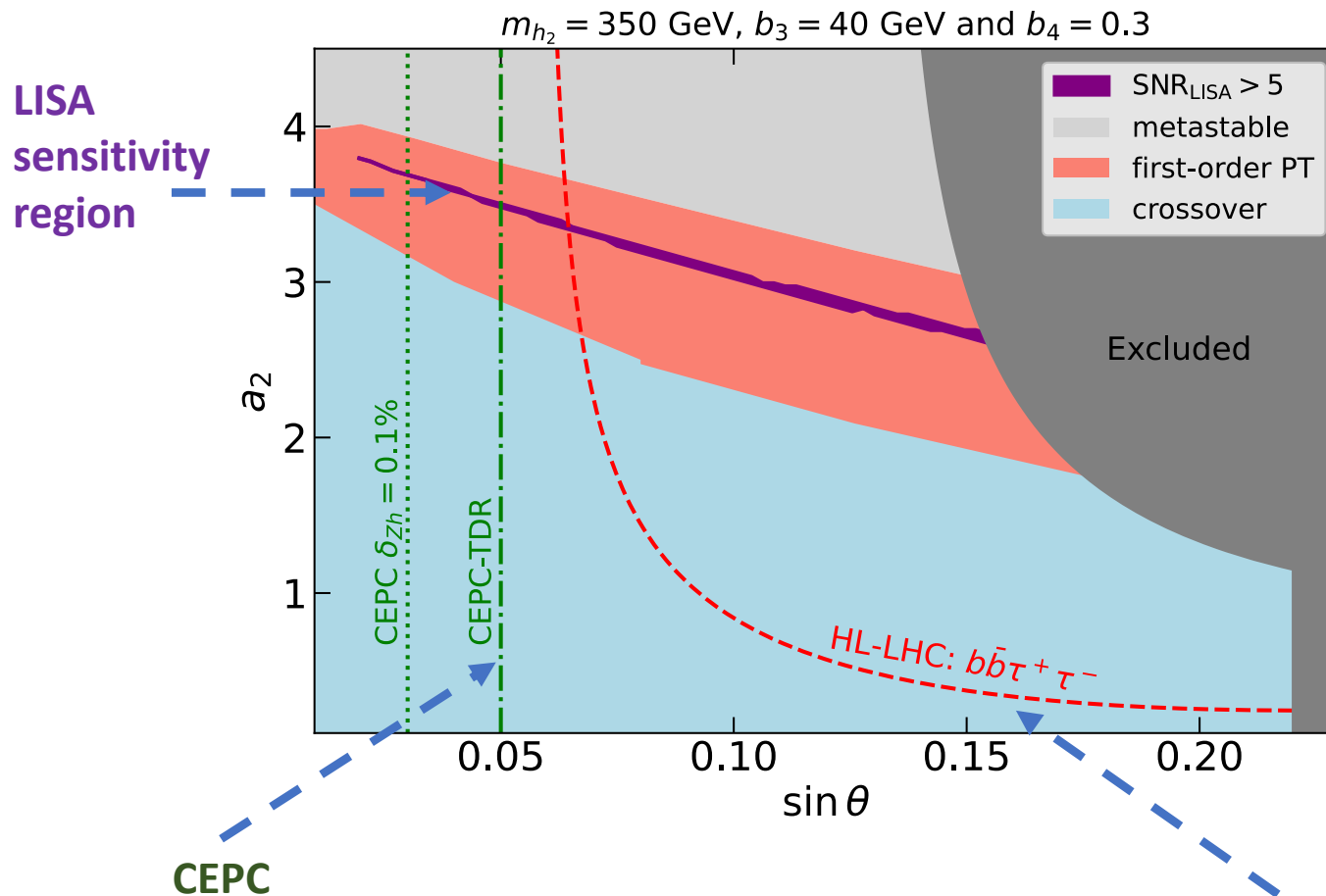


Ramsey-Musolf, Tenkanen, VQT: 2409.17554



- **Strong correlation** to nucleation temperature and the latent heat
- Lies in range of **[0.63, 0.85]** which corresponds to the **hybrids** profile solution for the wall where the wall has both a **rarefaction** and a **shock wave**!

Ramsey-Musolf, Tenkanen, VQT: 2409.17554



Di-Higgs searches at HL-LHC

Summary

- ❖ The first order electroweak phase transition is interesting and can be probed at future collider and GW detectors.
- ❖ We performed a cutting-edge analysis of GW prediction from the first-order EWPT, combining higher order corrections in perturbative calculations and results from lattice simulation
- ❖ We show a complementary between collider and GW signals in probing parameter space in xSM

Thank You

Back-up slide



1. Ensuring the **gauge invariance** for the effective potential:
 - High temperature expansion (**only LO**)
 - \hbar expansion (PRM) method [1] (possible to include **higher order corrections**)
2. Ensuring the **scale independence** <-- RG running for the couplings
3. Using dimensional reduction to obtain **3d-EFT**
 - a) **Thermal resummations** are systematically implemented
 - b) **Lattice simulation** results to determine the boundary for FOEWPT region
4. Building **high-loop effective potential** in 3d-EFT

[1]: H.H.Patel and M.J.Ramsey-Musolf JHEP 07 (2011), 029, arXiv:1101.4665

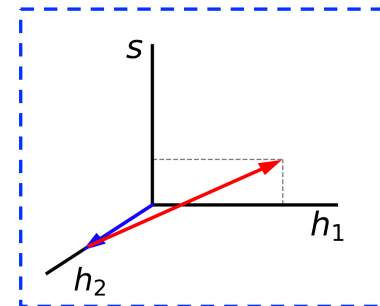
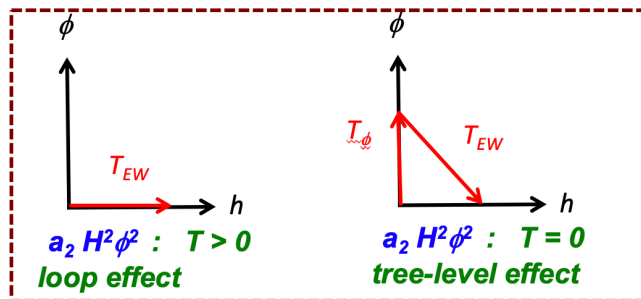
❖ Set scale for collider

$$V(h, T)_{\text{SM}} = D(T^2 - T_0^2) h^2 + \lambda h^4$$

$$T_0^2 = (8\lambda + \text{loops}) \left(4\lambda + \frac{3}{2}g^2 + \frac{1}{2}g'^2 + 2y_t^2 + \dots \right)^{-1} v^2$$

$$T_{\text{EW}} \equiv T_0 \approx 140 \text{ GeV}$$

❖ New scalar mass should **not be too heavy**



Mass new scalars < **700 GeV**

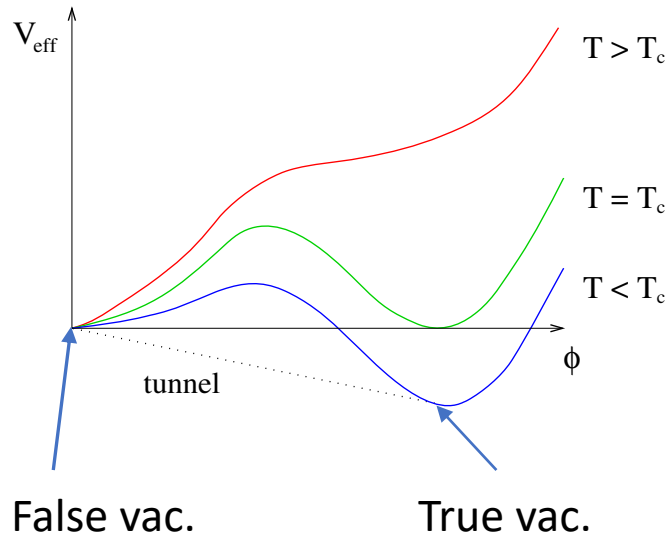
Michael J. Ramsey-Musolf: 1912.07189

Mass new scalars < **1.7 TeV**

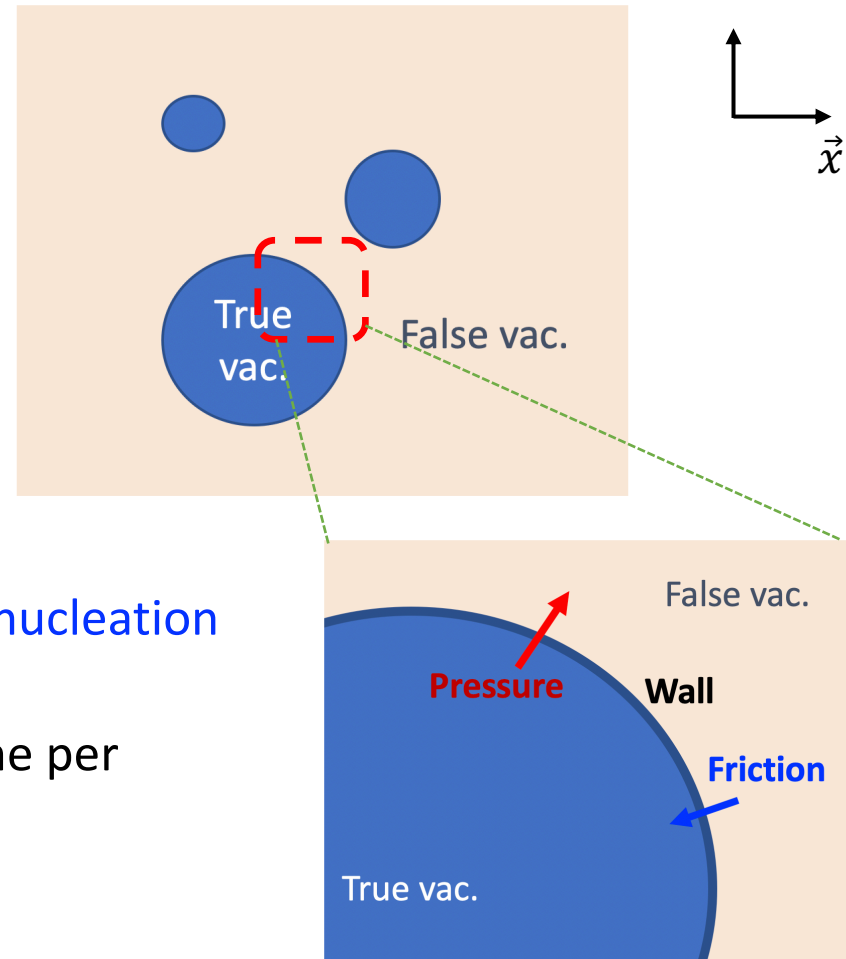
Michael J. Ramsey-Musolf, VQT and TC Yuan: 2408.05167

❖ **Modified the Higgs properties:**

Strong FOEWPT implies generics lower bound on mixing angle, exotic Higgs decays BR, $\Gamma(h \rightarrow \gamma\gamma)$



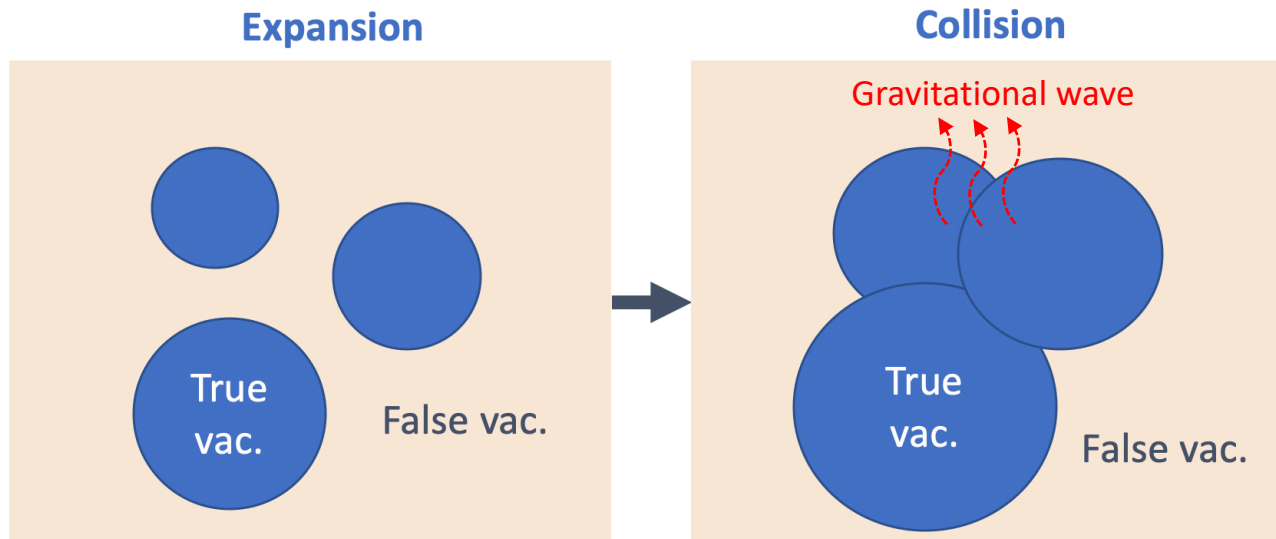
Bubble nucleation



- A 1st order phase transition proceeds by nucleation of bubbles.
- The bubble nucleation rate per unit volume per unit time

$$\Gamma(T) \simeq T^4 e^{-\frac{S_3(T)}{T}}$$

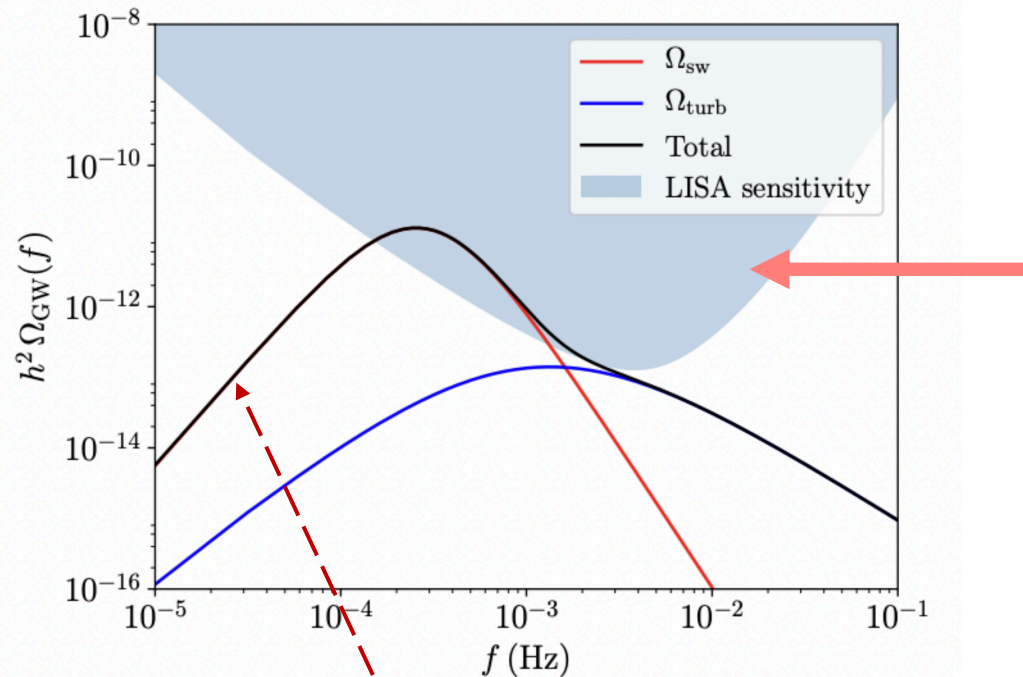
$S_3(T)$: the three dimensional Euclidean action



The kinetic energy of bubbles is transferred to GW either by:

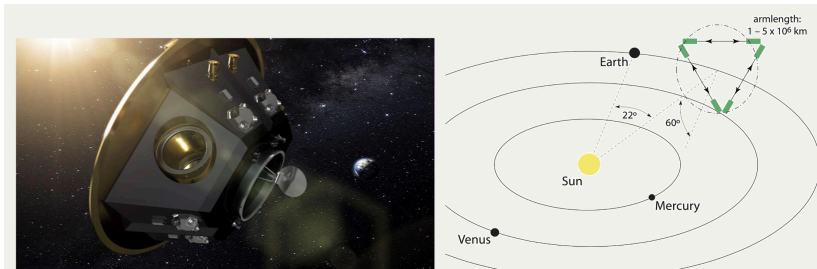
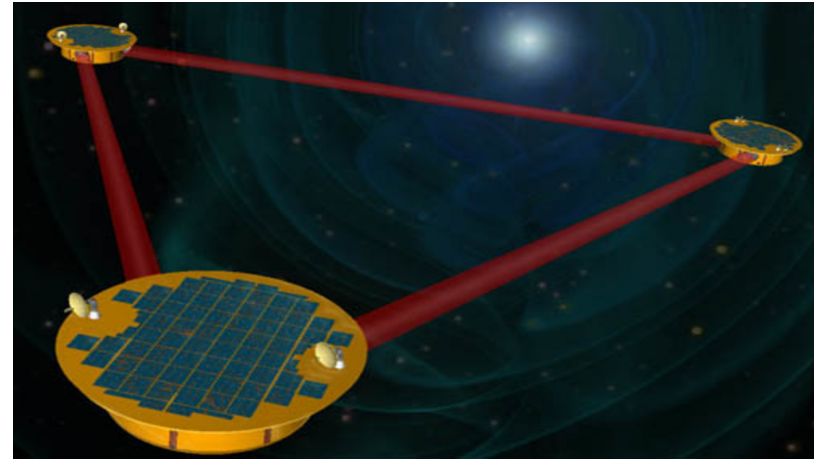
- Bubble collisions
- Injection of energy into the plasma fluid

Generating Gravitational Waves: detectable by LISA



GW spectrum from FOEWPT

LISA: Laser Interferometer Space Antenna



- Three laser arms, 2.5 M km separation
- ESA-NASA mission, launch by 2034
- Mission adopted 2017 [arXiv:1702.00786](https://arxiv.org/abs/1702.00786)



❖ Bosonic loop at $T > 0$

Bose distribution function

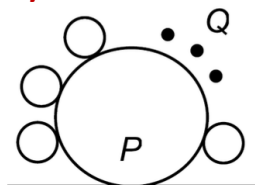


$$I(T) = g^2 \int \frac{d^3 p}{(2\pi)^3} f_B(E, T) \frac{1}{(p^2 + m^2)^n} \xrightarrow{\text{Small } p} \boxed{\frac{g^2 T}{m}} \int_{\text{I.R.}} \frac{d^3 p}{(2\pi)^3} \frac{1}{(p^2 + m^2)^n}$$

*Effective expansion **breaks down** if $m < g^2 T$*

❖ Field-dependent thermal mass:

Daisy resummation



$$m(\phi) = C_1 g^2 \phi^2$$



$$m(\phi, T) = C_1 g^2 \phi^2 + C_2 g^2 T^2$$

*Near the transition $\phi \rightarrow 0$,
thus I.R. sensitive near
phase trans*

Dimensional reduction

- ▶ Matsubara decomposition:

$$\phi(\tau, \mathbf{x}) = T \sum_n \tilde{\phi}(\mathbf{p}) e^{i\omega_n \tau}, \quad \omega_n = \begin{cases} 2\pi n T & \text{bosons} \\ (2n+1)\pi T & \text{fermions} \end{cases}$$

- ▶ Propagators: $\frac{1}{\mathbf{p}^2 + m^2 + \omega_n^2}$

- ▶ Modes with $n \neq 0$ are heavy and decouple at distances $\gg 1/T \rightarrow$ can be integrated out! (dimensional reduction)



Taken from Tuomas

DR: matching

Dimensional Reduction

All integrals are 3D with prefactor $T \rightarrow$ Rescale fields, couplings...

$$\int \frac{d^4 k}{(2\pi)^4} \rightarrow \frac{1}{\beta} \sum_n \int \frac{d^3 k}{(2\pi)^3}$$

- $\varphi_{4d}^2 = T \varphi_{3d}^2$
- $T \lambda_{4d} = \lambda_{3d}$

Thermal Loops

Equate Greens functions

$$\phi_{3d}^2 = \frac{1}{T} [1 + \hat{\Pi}'_{\phi}(0, 0)] \phi^2$$

Field

$$a_{2,3} = T [a_2 - a_2(\hat{\Pi}'_H(0) + \hat{\Pi}'_{\Sigma}(0)) + \hat{\Gamma}(0)]$$

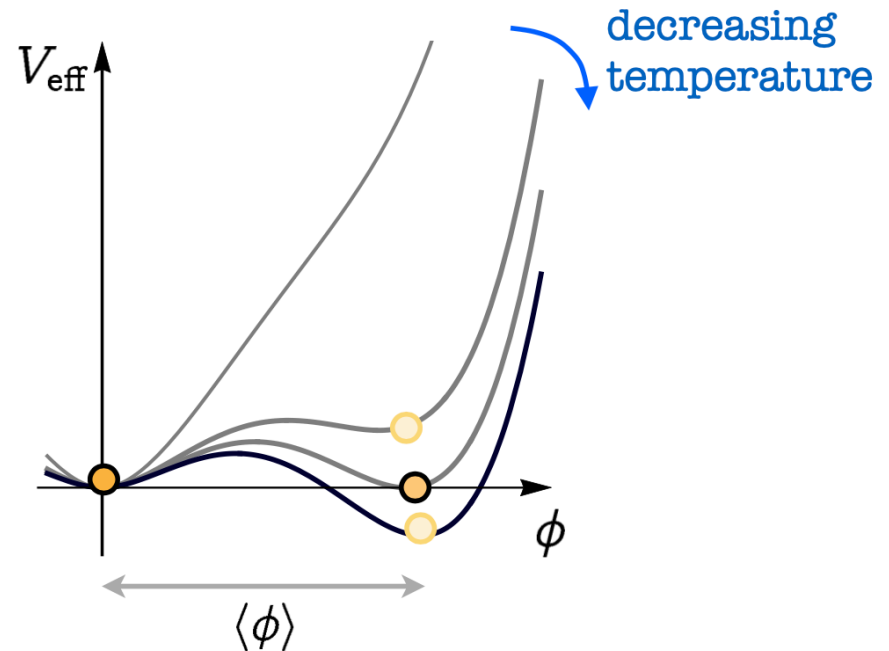
Quartic coupling

Gauge dependence issue

The standard method to compute ϕ_c/T_c is:

1. Track evolution of the minima in the V_{eff} as a function of temperature.
2. Solving the the minimization and degeneracy condition equations

$$\left\{ \begin{array}{l} \frac{\partial}{\partial \phi} V_{eff}(\phi_{min}, T_c) = 0 \\ V_{eff}(0, T_c) = V_{eff}(\phi_{min}, T_c) \end{array} \right.$$



Gauge dependence issue

However, in a gauge theory the V_{eff} is gauge dependent

For a general theory

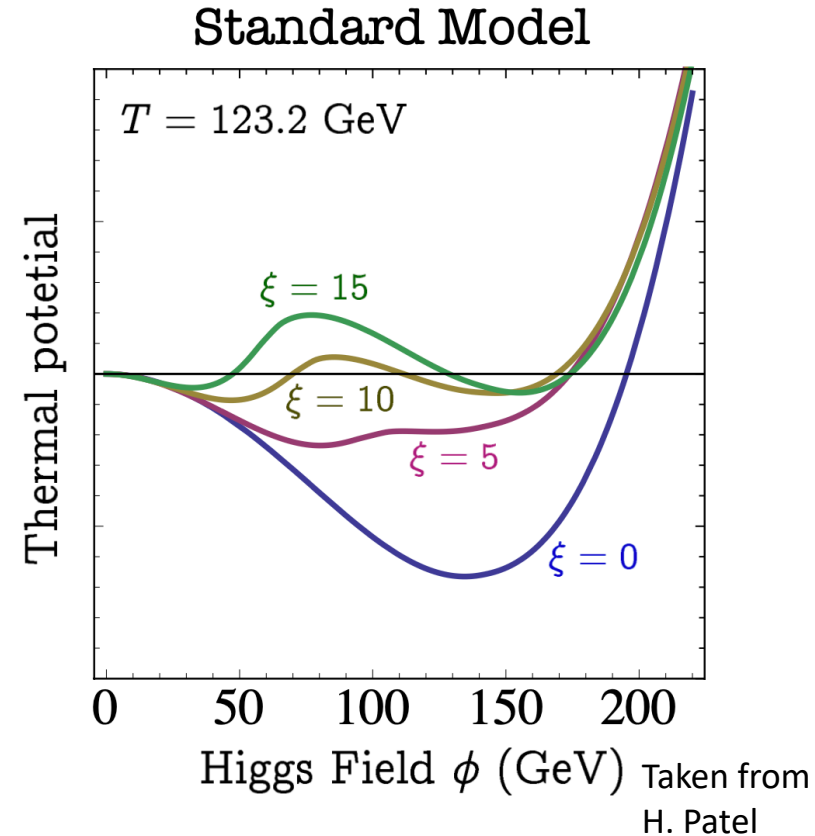
← $T = 0$

$$V_{eff}(\phi) = V_{tree}(\phi) + \sum_{\text{scalars}, i} \frac{1}{4(4\pi)^2} [\underline{m_i^2(\phi; \xi)}]^2 \left[\ln \left(\frac{m_i^2(\phi; \xi)}{\mu^2} \right) - \frac{3}{2} \right] + \sum_{\text{gauge}, a} \frac{3}{4(4\pi)^2} [m_a^2(\phi)]^2 \left[\ln \left(\frac{m_a^2(\phi)}{\mu^2} \right) - \frac{5}{6} \right] - \sum_{\text{gauge}, a} \frac{1}{4(4\pi)^2} [\underline{\xi m_a^2(\phi)}]^2 \left[\ln \left(\frac{\xi m_a^2(\phi)}{\mu^2} \right) - \frac{3}{2} \right],$$

← $T \neq 0$

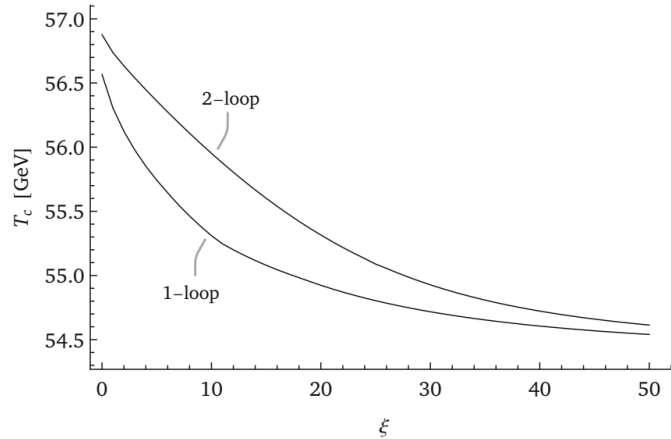
$$V_{eff}(\phi, T) = V_{eff}(\phi) + \frac{T^4}{2\pi^2} \left[\sum_{\text{scalar}, i} J_B(m_i^2(\phi; \xi)/T^2) + 3 \sum_{\text{gauge}, a} J_B(m_a^2(\phi)/T^2) - \sum_{\text{gauge}, a} J_B(\xi m_a^2(\phi)/T^2) \right]$$

Computed T_c and v_c depends on gauge parameter!

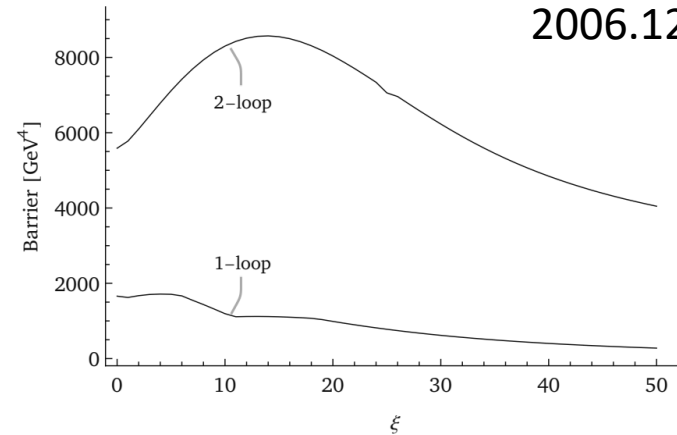


Gauge dependence issue

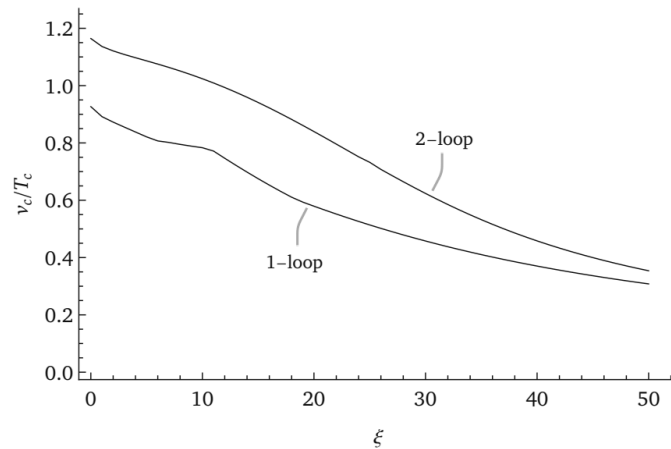
2006.12614



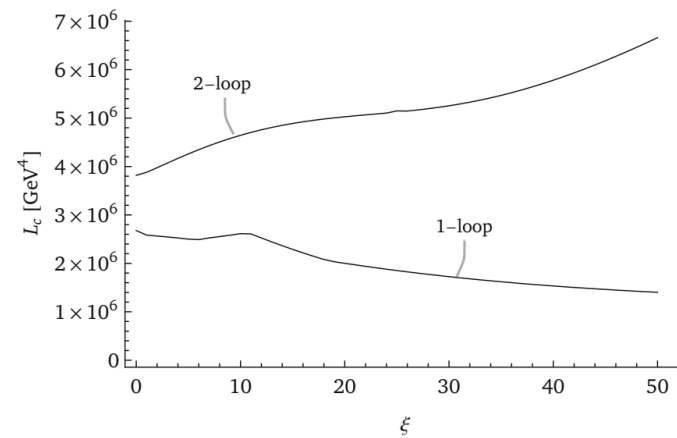
(a)



(b)



(c)



(d)

Resolution 1: high-T expansion

$$V_{\text{eff}}(\phi, T) = V_{\text{tree}}(\phi) + V_{\text{CW}}(\phi) + \frac{T^4}{2\pi^2} \left[\sum_{\text{scalar}, i} J_B(m_i^2(\phi; \xi)/T^2) + 3 \sum_{\text{gauge}, a} J_B(m_a^2(\phi)/T^2) - \sum_{\text{gauge}, a} J_B(\xi m_a^2(\phi)/T^2) \right]$$

High T expansion

$$V_{\text{eff}}(\phi, T) \approx V_{\text{tree}}(\phi) + V_{\text{CW}}(\phi) - \frac{\pi^2 T^4}{90} (n_s + 2n_g) + \frac{T^2}{24} \left[\sum_{\text{scalars}, i} m_i^2(\phi; \xi) + (3 - \xi) \sum_{\text{gauge}, a} m_a^2(\phi) \right]$$

$$- \frac{T}{12\pi} \left[\sum_{\text{scalars}, i} (m_i^2(\phi; \xi))^{3/2} + (3 - \xi^{3/2}) \sum_{\text{gauge}, a} (m_a^2(\phi))^{3/2} \right] - \frac{1}{64\pi^2} \left[\sum_{\text{scalars}, i} [m_i^2(\phi; \xi)]^2 \ln(m_i^2(\phi; \xi)/T^2) \right.$$

$$\left. + 3 \sum_{\text{gauge}, a} [m_a^2(\phi)]^2 \ln(m_a^2(\phi)/T^2) - \sum_{\text{gauge}, a} [\xi m_a^2(\phi)]^2 \ln(\xi m_a^2(\phi)/T^2) \right]$$

$$V_{\text{eff}}(\phi, T) \approx V_{\text{tree}}(\phi) + \frac{T^2}{24} \left[\text{Tr } M_{ij}^2(\phi) + 3 \text{Tr } m_A^2(\phi)^{ab} \right] - \frac{T}{12\pi} \left[\sum_{\text{scalars}, i} (m_i^2(\phi; \xi))^{3/2} + (3 - \xi^{3/2}) \sum_{\text{gauge}, a} (m_a^2(\phi))^{3/2} \right]$$

The effective potential is gauge independent if one takes the leading term T^2

Resolution 2: PRM method

- The Nielsen-Fukuda-Kugo identity

$$\frac{\partial V_{\text{eff}}(\varphi)}{\partial \xi} = -C(\varphi, \xi) \frac{\partial V_{\text{eff}}(\varphi)}{\partial \varphi},$$

- \hbar expansion for the effective potential and C

$$V_{\text{eff}}(\varphi) = V_0(\varphi) + \hbar V_1(\varphi) + \hbar^2 V_2(\varphi) + \dots,$$
$$C(\varphi, \xi) = c_0 + \hbar c_1(\varphi) + \hbar^2 c_2(\varphi) + \dots.$$

- Up to $O(\hbar)$, we have:

$$\frac{\partial V_1}{\partial \xi} = -c_1 \frac{\partial V_0}{\partial \varphi}.$$

→ the gauge dependence of V_1 **drops out** at the points where the **tree-level potential is extremized** (which differs from the extremum of V_1)

Resolution 2: PRM method

Up to two-loop expansion

$$\begin{aligned}
 V_{\text{eff}}^{\hbar} &= V_0 + \hbar V_1 + \hbar^2 V_2, \\
 \bar{v}_{\text{min}} &= \bar{v}_0 + \hbar \bar{v}_1 + \hbar^2 \bar{v}_2, \\
 \bar{s}_{\text{min}} &= \bar{s}_0 + \hbar \bar{s}_1 + \hbar^2 \bar{s}_2,
 \end{aligned}$$

where $\frac{\partial V_0}{\partial \bar{v}}|_{\bar{v}=\bar{v}_0} = 0$ and $\frac{\partial V_0}{\partial \bar{s}}|_{\bar{s}=\bar{s}_0} = 0$,

Satisfying Nielsen-Fukuda-Kugo identity \rightarrow gauge invariance

$$\begin{aligned}
 V_{\text{eff}}^{\hbar}(\bar{v}_{\text{min}}, \bar{s}_{\text{min}}) &= V_0(\bar{v}_0, \bar{s}_0) + \hbar V_1(\bar{v}_0, \bar{s}_0) \\
 &+ \hbar^2 \left[V_2(\bar{v}_0, \bar{s}_0) - \frac{1}{2} \bar{v}_1^2 \frac{\partial^2 V_0}{\partial \bar{v}^2} - \frac{1}{2} \bar{s}_1^2 \frac{\partial^2 V_0}{\partial \bar{s}^2} - \bar{v}_1 \bar{s}_1 \frac{\partial^2 V_0}{\partial \bar{v} \partial \bar{s}} \right] + \mathcal{O}(\hbar^3),
 \end{aligned} \tag{3.13}$$

where $\mathcal{O}(\hbar)$ corrections for the minima are given as

$$\bar{v}_1 = \left[\left(\frac{\partial^2 V_0}{\partial \bar{v} \partial \bar{s}} \right)^2 - \left(\frac{\partial^2 V_0}{\partial \bar{v}^2} \right) \left(\frac{\partial^2 V_0}{\partial \bar{s}^2} \right) \right]^{-1} \left[\left(\frac{\partial^2 V_0}{\partial \bar{s}^2} \right) \left(\frac{\partial V_1}{\partial \bar{v}} \right) - \left(\frac{\partial^2 V_0}{\partial \bar{v} \partial \bar{s}} \right) \left(\frac{\partial V_1}{\partial \bar{s}} \right) \right], \tag{3.14}$$

$$\bar{s}_1 = \left[\left(\frac{\partial^2 V_0}{\partial \bar{v} \partial \bar{s}} \right)^2 - \left(\frac{\partial^2 V_0}{\partial \bar{v}^2} \right) \left(\frac{\partial^2 V_0}{\partial \bar{s}^2} \right) \right]^{-1} \left[\left(\frac{\partial^2 V_0}{\partial \bar{v}^2} \right) \left(\frac{\partial V_1}{\partial \bar{s}} \right) - \left(\frac{\partial^2 V_0}{\partial \bar{v} \partial \bar{s}} \right) \left(\frac{\partial V_1}{\partial \bar{v}} \right) \right], \tag{3.15}$$

See 2103.07467 for expression of V_2

Resolution 2: PRM method

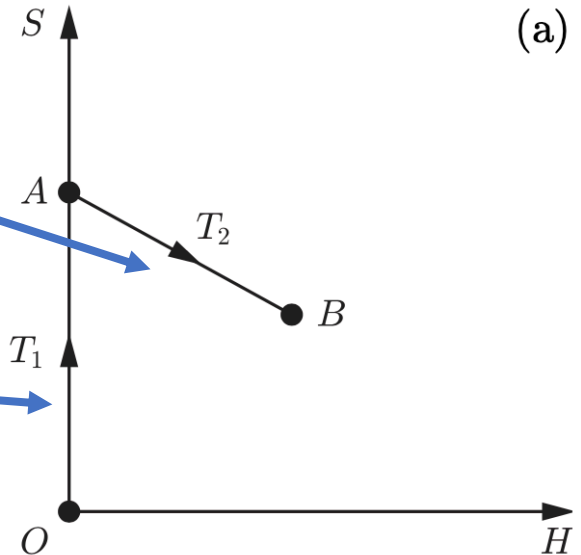
A. Determine T_c

A gauge independent way to compute T_c is by solving the **degeneracy condition** equation at **tree level extreme points**. For example for 2 step transition:

$$V_0(\mathbf{v}_0^A) + V_1(\mathbf{v}_0^A; T_C) = V_0(\mathbf{v}_0^B) + V_1(\mathbf{v}_0^B; T_C)$$

$$V_0(\mathbf{v}_0^A) + V_1(\mathbf{v}_0^A; T_C) = V_0(\mathbf{v}_0^O) + V_1(\mathbf{v}_0^O; T_C)$$

Where $\mathbf{v}_0^{A,B,O}$ are the **extreme points at tree level**.



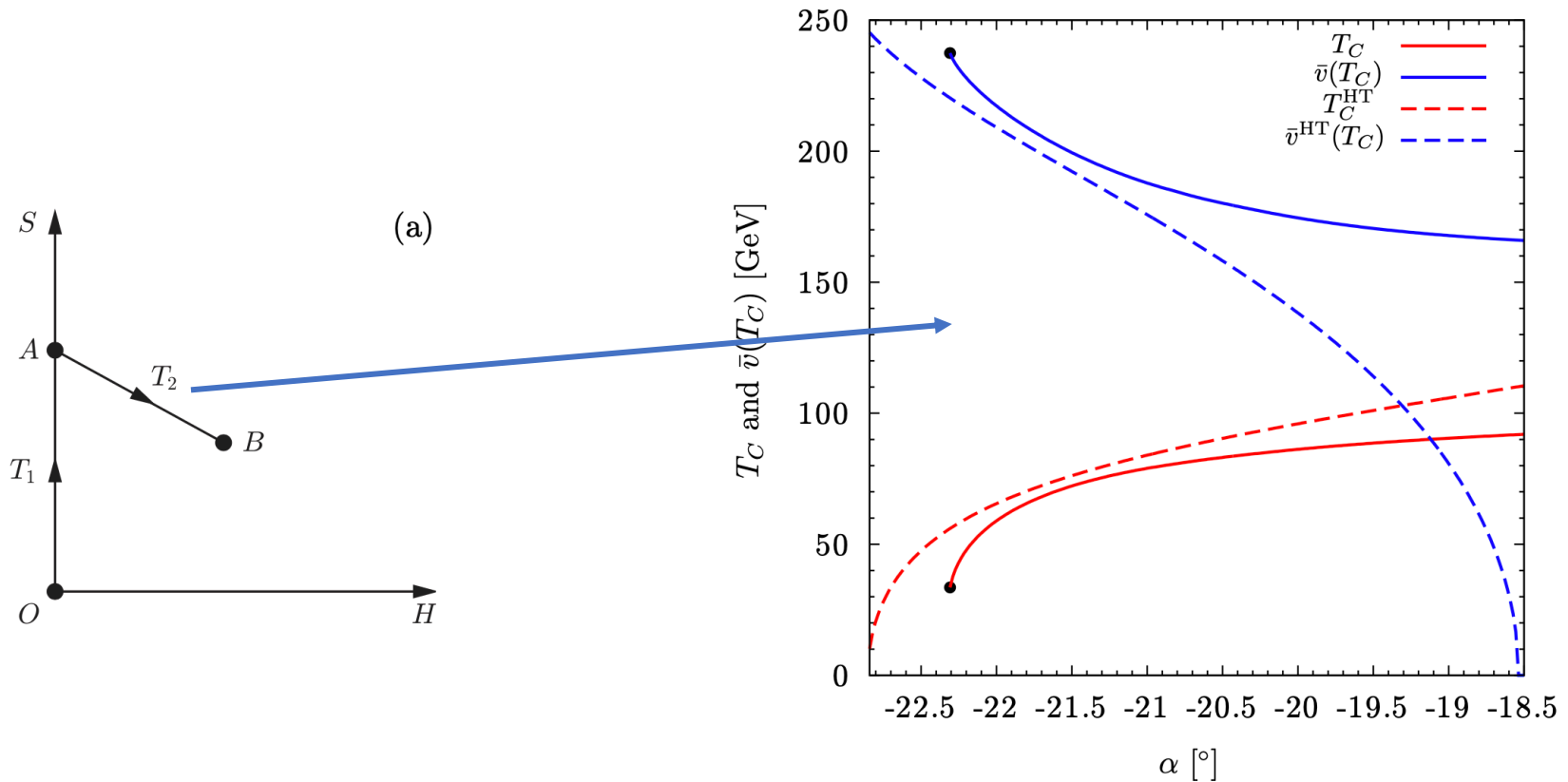
B. Determine v_c

v_c is computed by minimization of the high T effective potential at T_c

Resolution 2: PRM method

For complex scalar extension model

C. W. Chiang, M. J. Ramsey-Musolf and E. Senaha, Phys. Rev. D 97, no. 1, 015005 (2018)



Bubble nucleation and PT duration

- The first-order PT proceeds by bubble nucleation with a microscopic critical radius R_c .
- The nucleation rate per unit volume is

$$\mathcal{P} = A(t)e^{-S_c(t)}.$$

S_c is the critical bubble action which is the action for the smallest possible bubble able to expand

- The collisions of the bubbles, and the subsequent fluid flows, produce the shear stresses which source GWs.
- Below T_c the bubble action decreases from infinity and the nucleation probability increases rapidly. The rate of increase is defined:

$$\beta(T) = \frac{d}{dt} \ln \mathcal{P}(T)$$

- If $S_c \gg 1$ and $\beta \gg H$, we approximately obtain

$$\beta(T) = -dS_c/dt$$

Bubble nucleation and PT duration

- When the bubbles appear they grow due to a pressure difference between the interior and exterior.
- The onset of the PT is characterized by the nucleation of one bubble per horizon volume on average, which corresponds roughly to $S_c = 140$ for EWPT.
- As the bubbles grow and more appear, the fraction of the Universe in the metastable phase decreases extremely rapidly, leading to bubble percolation for the PT to successfully complete.
- For more precise value of S_c

$$S_c(\text{onset}) \simeq 141 + \log(A/T^4) - 4 \log\left(\frac{T}{100 \text{ GeV}}\right) - \log\left(\frac{\beta/H}{100}\right),$$

$$S_c(\text{percolation}) \simeq 131 + \log(A/T^4) - 4 \log\left(\frac{T}{100 \text{ GeV}}\right) - 4 \log\left(\frac{\beta/H}{100}\right) + 3 \log(v_w)$$

For EWPT:

$$\log(A/T^4) \simeq -14$$

B. Laurent and J.M. Cline: 2204.13120

W-Y. Ai, B. Laurent and J. Vis: 2303.10171

Stefania De Curtis et al. 2303.05846

Validity of the LTE approximation:

- Studies in xSM found that the wall velocities found with the **LTE** treatments only deviate by approximately **20%** from one taking into account the out-of-equilibrium effects
- However, these studies only explore the region of parameter space where the ratio of the **enthalpies** in the broken and symmetric phases, $\Psi > 0.9$.
- The out-of-equilibrium effects create an additional source of friction **slowing down the wall**, making the actual wall velocity smaller than what is predicted by the LTE assumption
- LTE can offer an **upper bound** for the wall velocity!

Bubble wall velocity in LTE



$$v_w^{\text{LTE}} = \left(\left| \frac{3\alpha + \Psi - 1}{2(2 - 3\Psi + \Psi^3)} \right|^{c/2} + \left| v_{\text{CJ}} \left(1 - a \frac{(1 - \Psi)^b}{\alpha} \right) \right|^c \right)^{1/c}. \quad (37)$$

Here $a = 0.2233$, $b = 1.074$, $c = -3.433$, $\Psi = \omega_t/\omega_f$ is the ratio of enthalpies and the Chapman–Jouguet velocity v_{CJ} is given by

$$v_{\text{CJ}} = \frac{1}{\sqrt{3}} \frac{1 + \sqrt{3\alpha^2 + 2\alpha}}{1 + \alpha}. \quad (38)$$

$$\alpha = \frac{4 [\theta_f(T) - \theta_t(T)]}{3\omega_f(T)} \Big|_{T=T_*}. \quad \leftarrow \text{Phase transition strength}$$

$$\omega(T) = T \frac{\partial p}{\partial T}, \quad \leftarrow \text{Enthalpy}$$

$$\theta(T) = \frac{1}{4} [\rho(T) - 3p], \quad \leftarrow \text{Trace anomaly}$$

$$p = \frac{\pi^2}{90} g_* T^4 - T V_{\text{eff}}^{\hbar}, \quad \leftarrow \text{Pressure}$$

EWPT: collider target

Michael J. Ramsey-Musolf: 1912.07189

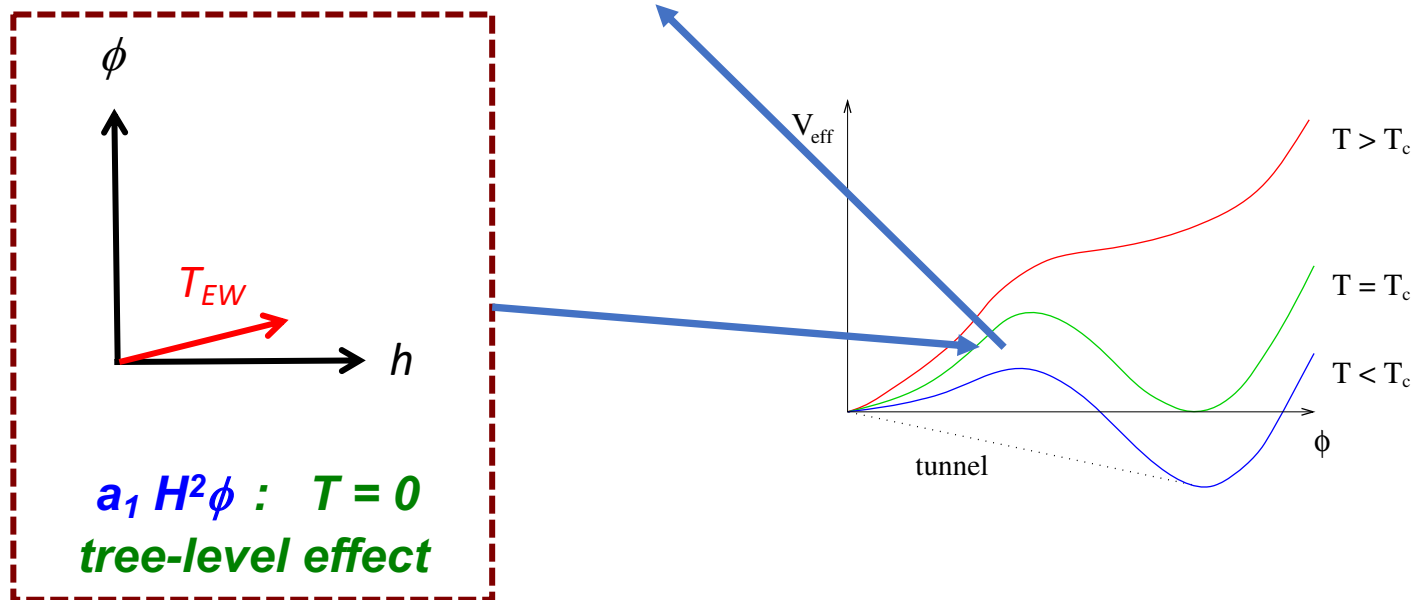
- For a strong 1st OEWPT: prevent baryon number washout

$$\frac{\bar{v}(T_{\text{EW}})}{T_{\text{EW}}}$$

$$\frac{|a_1|}{2\lambda T_{\text{EW}}} \gtrsim 1$$

$$|\sin \theta| \gtrsim 0.01$$

$$|\Delta\lambda/\lambda| \gtrsim 0.003$$





- Lagrangian

$$V(\phi, S) = \mu^2 \phi^\dagger \phi + \lambda (\phi^\dagger \phi)^2 + b_1 S + \frac{1}{2} b_2 S^2 + \frac{1}{3} b_3 S^3 + \frac{1}{4} b_4 S^4 + \frac{1}{2} a_1 S \phi^\dagger \phi + \frac{1}{2} a_2 S^2 \phi^\dagger \phi,$$

- Considering a scenario that Z_2 symmetry explicitly breaking and $\langle S \rangle = 0$ at zero temperature.

Mixing between h and S

$$\begin{pmatrix} h_1 \\ h_2 \end{pmatrix} = \begin{pmatrix} \cos \theta & -\sin \theta \\ \sin \theta & \cos \theta \end{pmatrix} \begin{pmatrix} h \\ S \end{pmatrix}$$

Parameter relations

$$\mu^2 = -\frac{1}{2} (m_{h_1}^2 \sin^2 \theta + m_{h_2}^2 \cos^2 \theta), \quad (4)$$

$$b_2 = m_{h_1}^2 \cos^2 \theta + m_{h_2}^2 \sin^2 \theta - a_2 v^2, \quad (5)$$

$$\lambda = -\frac{\mu^2}{v^2}, \quad (6)$$

$$a_1 = \frac{(m_{h_2}^2 - m_{h_1}^2) \sin 2\theta}{v}, \quad (7)$$

$$b_1 = -\frac{1}{4} v^2 a_1. \quad (8)$$

Thus the free parameters in the xSM are m_{h_2} , θ , a_2 , b_3 and b_4 .